PERGAMON International Journal of Non-Linear Mechanics 37 (2002) 1407–1419

INTERNATIONAL JOURNAL OF
NON-LINEAR
MECHANICS

www.elsevier.com/locate/ijnonlinmec

Random response of integrable Duhem hysteretic systems under non-white excitation

Y.Q. Ni[a,*], Z.G. Ying[b], J.M. Ko[a], W.Q. Zhu[b]

[a] *Department of Civil and Structural Engineering, The Hong Kong Polytechnic University, Hung Hom, Kowloon, Hong Kong*
[b] *Department of Mechanics, Zhejiang University, Hangzhou 310027, People's Republic of China*

Abstract

In this study, an integrable Duhem hysteresis model is derived from the mathematical Duhem operator. This model can represent a wide category of hysteretic systems. The stochastic averaging method of energy envelope is then adapted for response analysis of the integrable Duhem hysteretic system subjected to non-white random excitation. Using the integrability of the proposed model, potential energy and dissipated energy of the hysteretic system can be represented in an integration form so that the hysteretic restoring force is separable into conservative and dissipative parts. Based on the equivalence of dissipated energy, a non-hysteretic non-linear system is obtained to substitute the original system, and the averaged Itô stochastic differential equation of total energy is derived with the drift and diffusion coefficients being expressed as Fourier series expansions in space averaging. The stationary probability density of total energy and response statistics are obtained by solving the Fokker–Planck–Kolmogorov (FPK) equation associated with the Itô equation. Verification is given by comparing the computational results with Monte Carlo simulations.

Keywords: Hysteretic system; Integrable Duhem model; Random response; Stochastic averaging method

1. Introduction

Hysteresis phenomenon arises in many different areas of science and engineering, such as elastoplasticity, ferromagnetism, ferroelectricity, superconductivity, thermostats and shape-memory alloys. In structural dynamics field, the term hysteresis is used to describe a non-conservative system behaviour, in which the restoring force depends not only on the instantaneous deformation but also on the past history of deformation [1]. Structural systems under severe dynamic loading usually exhibit hysteretic behaviour, especially when the response becomes inelastic [2,3]. Meanwhile, a wide variety of hysteretic dampers have been devised and have found wide application in structural vibration control over the past two decades [4,5]. Recently, semi-active damping devices using smart materials such as shape-memory alloys, electro-rheological and magneto-rheological fluids have shown great promise for mitigating structural response subjected to seismic and wind excitation [6,7]. These smart materials also exhibit significant hysteresis behaviour.

Various analytical models have been proposed for describing hysteretic constitutive relationship, including bilinear and piecewise-linear models [8,9], Ramberg–Osgood model [10], Iwan's distributed element model [11], Bouc–Wen model [12,13],

* Corresponding author. Tel.: +852-2766-6004; fax: +852-2334-6389.
E-mail address: ceyqni@polyu.edu.hk (Y.Q. Ni).

0020-7462/02/$ - see front matter
PII: S0020-7462(02)00026-4

Ozdemir's model [14], Masing model [15], and so on. However, actual hysteretic phenomena arising in structural and mechanical systems are so complicated that there has been no well-accepted mathematical model which can describe all observed hysteretic characteristics. Some specific hysteresis features, e.g., soft-hardening hysteresis [16,17], non-local memory hysteresis [18,19], asymmetric hysteresis [20,21], are difficult to depict with fidelity by using the existing models.

Most dynamic loading on civil structures such as winds, earthquakes, waves is stochastic in nature. For strongly non-linear hysteretic systems, it is extremely difficult to obtain an exact analytical solution to a random response. The study of approximate solution techniques for random vibration analysis of hysteretic systems has been the focus of international research for several decades. Numerous investigations have been done by referring to the bilinear model, the distributed-element model and the Bouc–Wen model. The bilinear hysteretic systems were studied by the equivalent linearization techniques [22,23] and the stochastic averaging methods [1,24–26]. The distributed-element hysteretic systems were studied by the equivalent linearization techniques [27,28]. The Bouc–Wen hysteretic systems were studied by the equivalent linearization techniques [2,29–33] and the stochastic averaging methods [1,34,35]. It has been shown that for most cases the stochastic averaging methods, especially the quasi-conservative averaging and the stochastic averaging of energy envelope, gave more accurate results than the equivalent linearization techniques for both white noise excitation and non-stationary earthquake excitation.

Because of wide interests and obvious importance, the hysteresis phenomenon has been studied by mathematicians as a new branch of mathematics research [36]. They explored the hysteresis non-linearity in a purely mathematical form by introducing the concept of hysteresis operators. The hysteresis operators, e.g., Prandtl–Ishlinskii operator [37], Preisach operator [38] and Duhem operator [39], provide a powerful mathematical tool to describe and formulate generic hysteresis properties. It is highly desirable to develop analytical descriptions of observed hysteresis phenomena from this mathematical tool. In the present study, beginning with the mathematical Duhem operator, an integrable hysteresis model is constructed that possesses the following attributes: (i) the proposed model is versatile enough to cover most of the existing hysteresis models and to allow for the description of some specific hysteresis features; (ii) the proposed model is integrable so that the stochastic averaging methods can be applied. Subsequently, the stochastic averaging method of energy envelope is adapted for random vibration analysis of the integrable Duhem hysteretic systems under external and/or parametric non-white excitation. A space-averaging procedure instead of time averaging is formulated to evaluate the drift and diffusion coefficients associated with the derived Itô equation. Numerical examples and comparison with digital simulation results are given.

2. Integrable Duhem hysteresis model

Hysteresis is a special type of memory-based constitutive relation between input $x(t)$ and output $z(t)$, t being time. In the present study, $x(t)$ denotes displacement (strain) and $z(t)$ denotes restoring force (stress). Hysteresis appears when the output $z(t)$ is not uniquely determined by the input $x(t)$ at the same instant t, but instead $z(t)$ depends on the evolution of x in the interval $[0,t]$ and possibly also on the initial value z_0, namely

$$z(t) = \Gamma[x(\cdot), z_0](t), \tag{1}$$

where the memory-based functional $\Gamma[x(\cdot), z_0](t)$ is referred to as the hysteresis operator. The Duhem hysteresis operator establishes a mapping $\Gamma:(x, z_0) \mapsto z$ by postulating a Cauchy problem of the form [39]

$$\dot{z}(t) = g_1(x,z)\dot{x}_+(t) - g_2(x,z)\dot{x}_-(t), \tag{2a}$$

$$z(0) = z_0, \tag{2b}$$

where the over-dot denotes the time derivative; g_1 and g_2 are arbitrary continuous functions in the (x,z)-plane, and

$$\dot{x}_+(t) = \max[0, \dot{x}(t)] = \tfrac{1}{2}[|\dot{x}(t)| + \dot{x}(t)], \tag{3a}$$

$$\dot{x}_-(t) = -\min[0, \dot{x}(t)] = \tfrac{1}{2}[|\dot{x}(t)| - \dot{x}(t)]. \tag{3b}$$

The integrable Duhem hysteresis model is formulated by prescribing the ascending and descending

describing functions in the forms

$$g_1(x,z) = \frac{\mathrm{d}z_{01}(x)}{\mathrm{d}x} + h_{z1}(z - z_{01})h_{x1}(x), \tag{4a}$$

$$g_2(x,z) = \frac{\mathrm{d}z_{02}(x)}{\mathrm{d}x} + h_{z2}(z - z_{02})h_{x2}(x), \tag{4b}$$

where $z_{01}(x)$, $z_{02}(x)$, $h_{x1}(x)$, $h_{x2}(x)$, $h_{z1}(z - z_{01})$ and $h_{z2}(z - z_{02})$ are arbitrary continuous and differentiable functions.

Substituting Eqs. (4a) and (4b) into Eq. (2a) and integrating Eq. (2a) yields

$$G_{z1}(z - z_{01}) = G_{x1}(x), \quad \dot{x} \geqslant 0, \tag{5a}$$

$$G_{z2}(z - z_{02}) = G_{x2}(x), \quad \dot{x} < 0 \tag{5b}$$

in which,

$$G_{z1}(z - z_{01}) = \int_0^{z - z_{01}} \frac{\mathrm{d}u}{h_{z1}(u)}, \tag{6a}$$

$$G_{x1}(x) = \int_{-x_0}^{x} h_{x1}(u)\,\mathrm{d}u, \tag{6b}$$

$$G_{z2}(z - z_{02}) = \int_0^{z - z_{02}} \frac{\mathrm{d}u}{h_{z2}(u)}, \tag{6c}$$

$$G_{x2}(x) = \int_{x_0}^{x} h_{x2}(u)\,\mathrm{d}u, \tag{6d}$$

where x_0 is the residual hysteresis displacement that satisfies $z(x_0) = 0$ and $x_0 > 0$.

With Eqs. (5a) and (5b), the explicit expressions of ascending and descending curves of hysteresis loops can be obtained as

$$z(x) = z_1(x) = z_{01}(x) + G_{z1}^{-1}[G_{x1}(x)], \quad \dot{x} \geqslant 0, \tag{7a}$$

$$z(x) = z_2(x) = z_{02}(x) + G_{z2}^{-1}[G_{x2}(x)], \quad \dot{x} < 0. \tag{7b}$$

Most hysteretic systems exhibit symmetric hysteresis loops about the origin under symmetric loading sequence. For this kind of hysteresis, there is a generic relation $g_2(x,z) = g_1(-x,-z)$ [40], and the integrable Duhem hysteresis model is characterized only by the functions $z_0(x)$, $h_x(x)$ and $h_z(z - z_0)$. For example, for a symmetric hysteretic system with $h_z(z - z_0) = 1$ and

$$z_0(x) = \exp\left[\int f_1(x, \mathrm{sgn}(z_0))\,\mathrm{d}x\right] \times \left\{c + (1-n)\int f_2(x, \mathrm{sgn}(z_0)) \exp\left[(n-1) \times \int f_1(x, \mathrm{sgn}(z_0))\,\mathrm{d}x\right]\,\mathrm{d}x\right\}^{1/(1-n)}, \quad n \neq 1, \tag{8a}$$

$$z_0(x) = c \exp\left\{\int [f_1(x, \mathrm{sgn}(z_0)) + f_2(x, \mathrm{sgn}(z_0))]\,\mathrm{d}x\right\}, \quad n = 1 \tag{8b}$$

its ascending and descending describing functions are governed by

$$g_1(x,z) = h_x(x) + f_1(x, \mathrm{sgn}(z_0))z_0 + f_2(x, \mathrm{sgn}(z_0))z_0^n, \tag{9a}$$

$$g_2(x,z) = g_1(-x,-z) \tag{9b}$$

and the expressions of hysteresis loop curves are obtained as

$$z(x) = z_0(x) + G_{z1}^{-1}[G_{x1}(x)] = z_0(x) + \int h_x(x)\,\mathrm{d}x, \quad \dot{x} \geqslant 0, \tag{10a}$$

$$z(x) = -z_0(-x) - G_{z1}^{-1}[G_{x1}(-x)] = -z_0(-x) + \int h_x(-x)\,\mathrm{d}x, \quad \dot{x} < 0. \tag{10b}$$

The proposed integrable Duhem hysteresis model is a versatile model from which a wide category of differential-type hysteretic models existent in mechanical, structural and ferromagnetic disciplines can be derived. Derivation of these differential-type models from the integrable Duhem hysteresis model is given in Appendix A.

3. Random response analysis

3.1. Equivalent non-linearization

Consider an SDOF non-linear hysteretic system subjected to external and/or parametric random loading. The equation of motion of the system is of the form

$$\ddot{X} + 2\zeta\dot{X} + Z(X,\dot{X}) = f(X,\dot{X})\xi(t), \tag{11}$$

where X denotes non-dimensional displacement; ζ is viscous damping ratio; f represents the amplitude of excitation which is a continuous and differentiable function of displacement and velocity; $\xi(t)$ is wide-band stationary random excitation with zero mean. Z is a non-linear hysteretic restoring force governed by the integrable Duhem hysteresis model.

Let $z_1(x)$ and $z_2(x)$ be the ascending and descending curves of hysteresis loops, potential energy stored in the hysteresis component can be expressed as

$$U(x) = \int_{-x_0}^{x} z_1(x_1)\,\mathrm{d}x_1, \quad -a_1 \leqslant x \leqslant -x_0, \tag{12a}$$

$$U(x) = \int_{x_0}^{z_2^{-1}[z_1^{\mathrm{p}}(x)]} z_2(x_1)\,\mathrm{d}x_1, \quad -x_0 \leqslant x \leqslant a_2, \tag{12b}$$

where $-a_1$ and a_2 are the negative and positive displacement amplitudes; x_0 is the residual hysteresis displacement; superscript p denotes the inelastic part of hysteretic restoring force.

The total energy of the hysteretic system (11) is given by

$$H = \dot{x}^2/2 + U(x). \tag{13}$$

Energy dissipated in one cycle by the hysteresis component is equal to the area of hysteresis loop, namely,

$$A_r = \oint z(x)\,\mathrm{d}x = \int_{-a_1}^{a_2} z_1(x)\,\mathrm{d}x + \int_{a_2}^{-a_1} z_2(x)\,\mathrm{d}x. \tag{14}$$

For a symmetric hysteresis system, there holds $z_1(x) = -z_2(-x)$, $a_1 = a_2 = a$. In this case, after separating the hysteretic force into elastic and inelastic parts ($z_1 = z^{\mathrm{e}} + z_1^{\mathrm{p}}$, $z_2 = z^{\mathrm{e}} + z_2^{\mathrm{p}}$), the potential energy and the dissipated energy can be expressed as

$$U(x) = \int_0^x z^{\mathrm{e}}(x_1)\,\mathrm{d}x_1 + \int_{-x_0}^{x} z_1^{\mathrm{p}}(x_1)\,\mathrm{d}x_1, \quad -a \leqslant x \leqslant -x_0, \tag{15a}$$

$$U(x) = \int_0^x z^{\mathrm{e}}(x_1)\,\mathrm{d}x_1 + \int_{x_0}^{(z_2^{\mathrm{p}})^{-1}[z_1^{\mathrm{p}}(x)]} z_2^{\mathrm{p}}(x_1)\,\mathrm{d}x_1, \quad -x_0 \leqslant x \leqslant a, \tag{15b}$$

$$A_r = \oint z^{\mathrm{p}}(x)\,\mathrm{d}x = 2\int_{-a}^{a} z_1(x)\,\mathrm{d}x, \tag{16}$$

where a is determined by solving $H = U(a)$.

It is impossible at present to obtain an exact analytical solution to a random response of system (11). The equivalent non-linearization technique [1,24,41] is utilized here to approximate the hysteresis damping by quasi-linear non-hysteretic damping in terms of equivalent energy dissipation. After doing this, the integrable Duhem hysteretic system (11) can be replaced by the following equivalent non-linear non-hysteretic system:

$$\ddot{X} + [2\zeta + 2\zeta_1(H)]\dot{X} + \partial U(X)/\partial X = f(X,\dot{X})\xi(t) \tag{17}$$

in which the coefficient of equivalent damping is obtained as a function of total energy in the following form:

$$2\zeta_1(H) = \frac{A_r}{2\int_{-a_1}^{a_2}\sqrt{2H - 2U(x)}\,\mathrm{d}x}, \tag{18}$$

where, for a general asymmetric oscillator, a_1 is determined by solving $H = U(-a_1)$ using Eq. (12a) and a_2 is determined by solving $H = U(a_2)$ using Eq. (12b).

3.2. Stochastic average method

The equivalent non-linear non-hysteretic system (17) is subjected to non-white random excitation. The stochastic averaging method [24,34,42,43] is applied here to obtain the FPK equation associated with the averaged Itô stochastic differential equation of total energy. Letting

$$\mathrm{sgn}(X)\sqrt{U(X)} = \sqrt{H}\cos\varphi, \quad \dot{X} = -\sqrt{2H}\sin\varphi \quad 0 \leqslant \varphi < 2\pi. \tag{19}$$

Eq. (17) is transformed as two first-order differential equations of total energy and phase as follows:

$$\dot{H} = -2H\sin^2\varphi[2\zeta + 2\zeta_1(H)] - \sqrt{2H}\sin\varphi\, f(H,\varphi)\xi(t), \tag{20a}$$

$$\dot{\varphi} = \frac{1}{\sqrt{2H}}\left[-\sqrt{2H}\sin\varphi\cos\varphi(2\zeta + 2\zeta_1(H)) + \frac{\partial U(X)/\partial X}{\cos\varphi}\right] - \frac{\cos\varphi}{\sqrt{2H}} f(H,\varphi)\xi(t), \tag{20b}$$

$$f(H,\varphi) = f[H(X,\dot{X}),\varphi(X,\dot{X})]. \tag{20c}$$

The total energy is approximated as a Markov diffusion process under the condition that damping and excitation are weak. Assuming that the total energy is a slowly varying process, time averaging can be made

to yield the following Itô equation:

$$\mathrm{d}H = m(H)\,\mathrm{d}t + \sigma(H)\,\mathrm{d}B(t), \tag{21}$$

where $B(t)$ is unit Wiener process; and

$$\begin{aligned} m(H) = \Big\langle & -2H\sin^2\varphi[2\zeta + 2\zeta_1(H)] \\ & + \int_{-\infty}^{0} [(\sqrt{2H}\sin\varphi f(H,\varphi))_{t+\tau} \\ & \times \frac{\partial}{\partial H}(\sqrt{2H}\sin\varphi f(H,\varphi))_t \\ & + \left(\frac{\cos\varphi}{\sqrt{2H}} f(H,\varphi)\right)_{t+\tau} \\ & \times \frac{\partial}{\partial\varphi}(\sqrt{2H}\sin\varphi f(H,\varphi))_t]R(\tau)\,\mathrm{d}\tau \Big\rangle_t, \end{aligned} \tag{22a}$$

$$\begin{aligned} \sigma^2(H) = \Big\langle & \int_{-\infty}^{+\infty} (\sqrt{2H}\sin\varphi f(H,\varphi))_{t+\tau} \\ & \times (\sqrt{2H}\sin\varphi f(H,\varphi))_t R(\tau)\,\mathrm{d}\tau \Big\rangle_t, \end{aligned} \tag{22b}$$

where $\langle\cdot\rangle_t$ represents time averaging, and $R(\tau) = E[\xi(t)\xi(t+\tau)]$ is the correlation function. For a fixed H, X and $\dot{X}$ can be treated as periodic functions, and consequently the following Fourier series expansions can be obtained:

$$\sin\varphi f(H,\varphi) = \frac{a_0^{(1)}}{2} + \sum_{i=1}^{\infty}\left(a_i^{(1)}\cos\frac{2\pi i t}{T} + a_i^{(2)}\sin\frac{2\pi i t}{T}\right), \tag{23a}$$

$$\cos\varphi f(H,\varphi) = \frac{b_0^{(1)}}{2} + \sum_{i=1}^{\infty}\left(b_i^{(1)}\cos\frac{2\pi i t}{T} + b_i^{(2)}\sin\frac{2\pi i t}{T}\right), \tag{23b}$$

$$2H\sin\varphi\frac{\partial f(H,\varphi)}{\partial H} = \frac{c_0^{(1)}}{2} + \sum_{i=1}^{\infty}\left(c_i^{(1)}\cos\frac{2\pi i t}{T} + c_i^{(2)}\sin\frac{2\pi i t}{T}\right), \tag{23c}$$

$$\sin\varphi\frac{\partial f(H,\varphi)}{\partial\varphi} = \frac{d_0^{(1)}}{2} + \sum_{i=1}^{\infty}\left(d_i^{(1)}\cos\frac{2\pi i t}{T} + d_i^{(2)}\sin\frac{2\pi i t}{T}\right), \tag{23d}$$

where the coefficients $a_i^{(k)}$, $b_i^{(k)}$, $c_i^{(k)}$ and $d_i^{(k)}$ $(k=1,2)$ are given in Appendix B.

By substituting Eq. (23) into Eq. (22), the averaged drift and diffusion coefficients are obtained as

$$\begin{aligned} m(H) = & -\frac{A_r}{T} - \frac{4\zeta}{T}\int_{-a_1}^{a_2}\sqrt{2H - 2U(x)}\,\mathrm{d}x \\ & + \frac{\pi}{4}(a_0^{(1)}a_0^{(1)} + a_0^{(1)}c_0^{(1)} + b_0^{(1)}b_0^{(1)} \\ & + b_0^{(1)}d_0^{(1)})\Phi_1(0) + \frac{\pi}{2}\sum_{i=1}^{\infty}[(a_i^{(1)}a_i^{(1)} \\ & + a_i^{(2)}a_i^{(2)} + a_i^{(1)}c_i^{(1)} + a_i^{(2)}c_i^{(2)} \\ & + b_i^{(1)}b_i^{(1)} + b_i^{(2)}b_i^{(2)} + b_i^{(1)}d_i^{(1)} \\ & + b_i^{(2)}d_i^{(2)})\Phi_1(2\pi i/T) + (a_i^{(2)}c_i^{(1)} - a_i^{(1)}c_i^{(2)} \\ & + b_i^{(2)}d_i^{(1)} - b_i^{(1)}d_i^{(2)})\Phi_2(2\pi i/T)] \end{aligned} \tag{24a}$$

$$\begin{aligned} \sigma^2(H) = & \pi H a_0^{(1)}a_0^{(1)}\Phi_1(0) \\ & + 2\pi H\sum_{i=1}^{\infty}[(a_i^{(1)}a_i^{(1)} + a_i^{(2)}a_i^{(2)})\Phi_1(2\pi i/T)], \end{aligned} \tag{24b}$$

where

$$\Phi_1(\omega) = \frac{1}{\pi}\int_{-\infty}^{0} R(\tau)\cos\omega\tau\,\mathrm{d}\tau, \tag{25a}$$

$$\Phi_2(\omega) = \frac{1}{\pi}\int_{-\infty}^{0} R(\tau)\sin\omega\tau\,\mathrm{d}\tau. \tag{25b}$$

The FPK equation associated with the averaged Itô equation of total energy is

$$\frac{\partial p}{\partial t} + \frac{\partial}{\partial H}[m(H)p] - \frac{1}{2}\frac{\partial^2}{\partial H^2}[\sigma^2(H)p] = 0, \tag{26}$$

where the probability density is $p = p(H,t)$ with initial condition $p(H_0,t_0)$ or $p = p(H,t|H_0,t_0)$. with initial condition $p = \delta(H - H_0)$. The stationary probability density of total energy can be obtained from Eq. (26) by imposing $\partial p/\partial t = 0$ as follows:

$$p(H) = \frac{C}{\sigma^2(H)} \exp\left\{\int_0^H \frac{2m(y)}{\sigma^2(y)}\,\mathrm{d}y\right\}, \tag{27}$$

where C is a normalizing constant. The mean square displacement is then calculated by

$$E[X^2] = \int_0^\infty \frac{p(H)}{T(H)}\,\mathrm{d}H \times 2\int_{-a_1}^{a_2} \frac{x^2\,\mathrm{d}x}{\sqrt{2H - 2U(x)}}. \tag{28}$$

4. Case study

To illustrate the proposed method, consider a non-linear hysteretic system subjected to external and parametric random loading. The equation of motion is expressed as

$$\ddot{X} + 2\zeta\dot{X} + Z(X,\dot{X}) = (e_1 + e_2X)\xi(t), \tag{29}$$

where e_1 and e_2 are constants; $\xi(t)$ is a non-white stationary excitation with the Kanai–Tajimi spectral density

$$\Phi_1(\omega) = \frac{1 + 4\zeta_g^2(\omega/\omega_g)^2}{[1 - (\omega/\omega_g)^2]^2 + 4\zeta_g^2(\omega/\omega_g)^2}\,S_0 \tag{30}$$

in which S_0 represents the excitation intensity; ω_g and ζ_g are the natural frequency and damping ratio of the excitation filter.

In this example, the ascending and descending describing functions of the integrable Duhem hysteresis model are taken as the form

$$g_1(x,z) = k_1 + 3k_3x^2 + \frac{\gamma}{\beta} - \gamma(z - k_1x - k_3x^3), \tag{31a}$$

$$g_2(x,z) = g_1(-x,-z), \tag{31b}$$

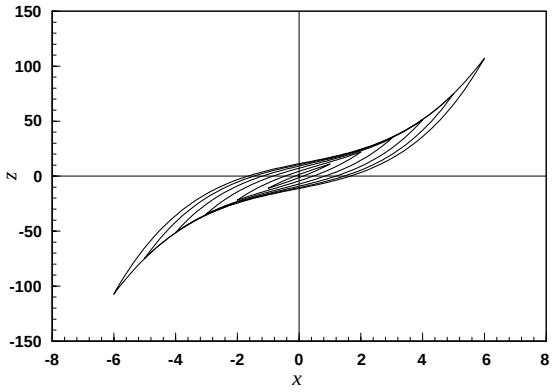

Fig. 1. Hardening hysteresis loops represented by integrable Duhem model ($k_1 = 5.0$, $k_3 = 0.3$, $\beta = 0.08$, $\gamma = 0.5$).

which correspond to

$$z_0(x) = k_1x + k_3x^3, \tag{32a}$$

$$h_x(x) = 1, \tag{32b}$$

$$h_z(z - z_0) = \frac{\gamma}{\beta} - \gamma(z - z_0). \tag{32c}$$

Figs. 1–3 show the hysteresis loops represented by the integrable Duhem hysteresis model in terms of Eq. (31) under different parameter combinations. It is seen that by selecting proper parameters, the integrable Duhem hysteresis model can represent a wide variety of hardening, softening, and soft-hardening hysteresis. It should be noted that the soft-hardening hysteresis is very difficult to depict by means of the existing differential-type models. These illustrations demonstrate that the presented model is a universal hysteresis model.

With the describing functions given in Eq. (31), the hysteresis loop curves are determined as

$$z = z_1 = k_1x + k_3x^3 + \frac{1}{\beta}[1 - \mathrm{e}^{-\gamma(x+x_0)}], \quad \dot{x} \geqslant 0, \tag{33a}$$

$$z = z_2 = k_1x + k_3x^3 - \frac{1}{\beta}[1 - \mathrm{e}^{\gamma(x-x_0)}], \quad \dot{x} < 0 \tag{33b}$$

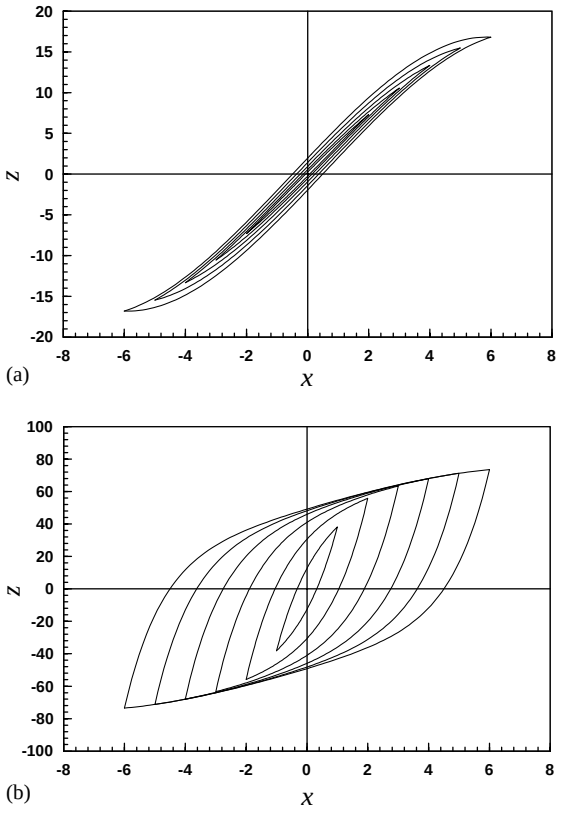

Fig. 2. Softening hysteresis loops represented by integrable Duhem model (a) $k_1 = 5.0$, $k_3 = -0.03$, $\beta = -0.08$, $\gamma = 0.1$; (b) $k_1 = 5.0$, $k_3 = -0.03$, $\beta = 0.02$, $\gamma = 0.8$.

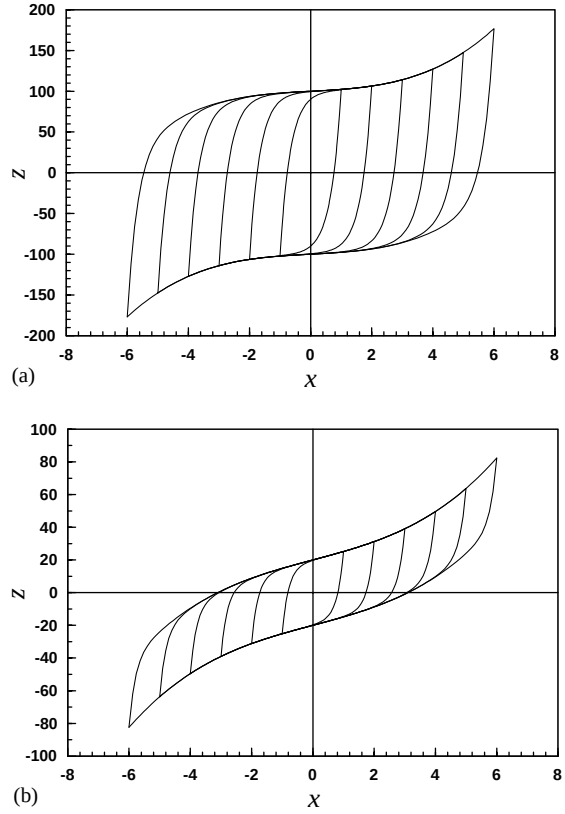

Fig. 3. Soft-hardening hysteresis loops represented by integrable Duhem model (a) $k_1 = 2.0$, $k_3 = 0.3$, $\beta = 0.01$, $\gamma = 3.0$; (b) $k_1 = 5.0$, $k_3 = 0.15$, $\beta = 0.05$, $\gamma = 5.0$.

and the potential energy and the dissipated energy in one cycle by the hysteresis component are obtained as

$$U(x) = \frac{1}{2}k_1x^2 + \frac{1}{4}k_3x^4 + \frac{1}{\beta}(x + x_0) + \frac{1}{\beta\gamma}[e^{-\gamma(x+x_0)} - 1], \quad -a \leqslant x \leqslant -x_0, \tag{34a}$$

$$U(x) = \frac{1}{2}k_1x^2 + \frac{1}{4}k_3x^4 + \frac{1}{\beta\gamma}[1 - e^{-\gamma(x+x_0)}] - \frac{1}{\beta\gamma}\ln[2 - e^{-\gamma(x+x_0)}], \quad -x_0 \leqslant x \leqslant a, \tag{34b}$$

$$A_r = \frac{4}{\beta\gamma}(1 + a\gamma) - \frac{4}{\beta\gamma}e^{\gamma(a-x_0)}, \tag{35}$$

where the residual hysteresis displacement x_0 and the displacement amplitude a for a given H are determined by

$$x_0 = -a + \frac{1}{\gamma}\ln\frac{1 + e^{2a\gamma}}{2}, \tag{36a}$$

$$H = \frac{1}{2}k_1a^2 + \frac{1}{4}k_3a^4 - \frac{1}{\beta}(a - x_0) + \frac{1}{\beta\gamma}[e^{\gamma(a-x_0)} - 1]. \tag{36b}$$

The averaged Itô stochastic differential equation is in the form of Eq. (21), where the drift and diffusion

coefficients are, respectively,

$$m(H) = -\frac{A_r}{T} - \frac{4\zeta}{T}\int_{-a}^{a}\sqrt{2H-2U(x)}\,\mathrm{d}x + \frac{\pi}{4}b_0^{(1)}b_0^{(1)}\Phi_1(0) + \frac{\pi}{2}\sum_{i=1}^{\infty}[a_i^{(2)}a_i^{(2)}+b_i^{(1)}b_i^{(1)}]\Phi_1\left(\frac{2\pi i}{T}\right), \tag{37a}$$

$$\sigma^2(H) = 2\pi H\sum_{i=1}^{\infty}a_i^{(2)}a_i^{(2)}\Phi_1\left(\frac{2\pi i}{T}\right) \tag{37b}$$

in which the Fourier expansion coefficients are given by

$$a_i^{(2)} = -\frac{2\sqrt{2}}{T\sqrt{H}}\int_{-a}^{a}\sin\left[\frac{2\pi i}{T}\times\int_{-a}^{x}\frac{\mathrm{d}x_1}{\sqrt{2H-2U(x_1)}}\right]\mathrm{d}x, \tag{38a}$$

$$b_i^{(1)} = \frac{4}{T\sqrt{H}}\int_{-a}^{a}\frac{\mathrm{sgn}(x)\sqrt{U(x)}}{\sqrt{2H-2U(x)}}\times\cos\left[\frac{2\pi i}{T}\int_{-a}^{x}\frac{\mathrm{d}x_1}{\sqrt{2H-2U(x_1)}}\right]\mathrm{d}x. \tag{38b}$$

With the above expressions, the stationary probability density of Eq. (27) is obtained by solving the FPK equation associated with the averaged Itô equation, and then the mean square displacement response is evaluated from Eq. (28).

To verify the accuracy of the proposed method, numerical computational results are obtained and compared with direct digital simulation. The following parameter values are taken in the computation: $\zeta = 0.2$, k_1=5.0 or 2.0, k_3=0.03, S_0=1.0, ω_g=3.08, ζ_g= 0.1. Fig. 4 illustrates the hysteresis loops produced by taking k_1=5.0, k_3=0.03, β=0.1 and γ=3.0, which are a good representation of the experimental hysteresis loops of a friction-type vibration isolator [40]. Figs. 5 and 6 show the corresponding Fourier expansion coefficients $a_i^{(2)}$ and $b_i^{(1)}$ ($i = 0, 1, 2, 3$) of the drift and diffusion coefficients versus total energy H. It is found that these coefficients for $i \neq 1$ are much smaller than those for $i = 1$ and decrease with the increasing order i. Only the first three order Fourier expansion coefficients are retained in the computation.

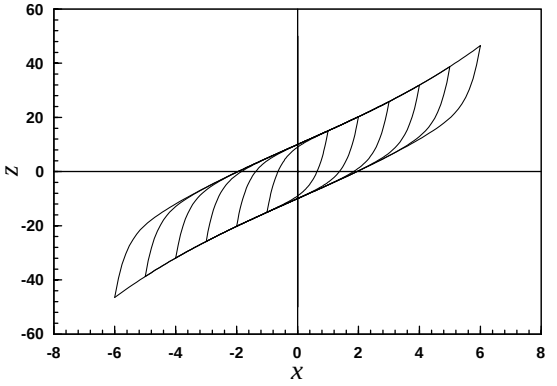

Fig. 4. Hysteresis loops of an isolator represented by integrable Duhem model ($k_1 = 5.0$, $k_3 = 0.03$, $\beta = 0.1$, $\gamma = 3.0$).

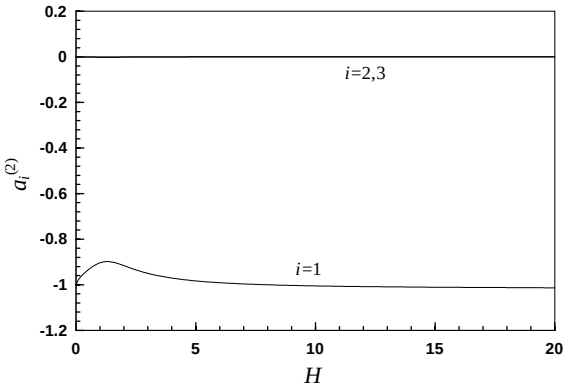

Fig. 5. Fourier coefficients $a_i^{(2)}$ versus total energy H ($k_1 = 5.0$, $k_3 = 0.03$, $\beta = 0.1$, $\gamma = 3.0$).

Two excitation cases are addressed. The first case corresponds to a purely external excitation with the parameters $e_1 = 1.0$ and $e_2 = 0.0$. Under this external excitation, the mean square displacements obtained by the proposed method (solid line) and by the direct digital simulation (dot) are obtained and shown in Figs. 7 and 8 for different excitation intensities and different excitation filter frequencies, respectively. It is seen that the mean square displacement response increases with the random excitation intensity, and there is a peak response within the frequency range of

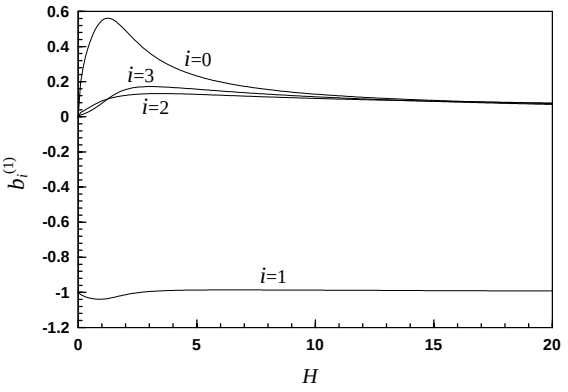

Fig. 6. Fourier coefficients $b_i^{(1)}$ versus total energy H ($k_1 = 5.0$, $k_3 = 0.03$, $\beta = 0.1$, $\gamma = 3.0$).

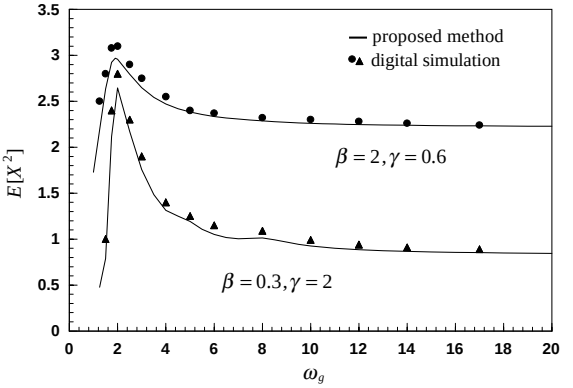

Fig. 8. Mean square displacement response versus excitation filter frequency ($e_1 = 1.0$, $e_2 = 0.0$, $\zeta = 0.2$, $k_1 = 2.0$, $k_3 = 0.03$, $S_0 = 1.0$, $\zeta_g = 0.1$).

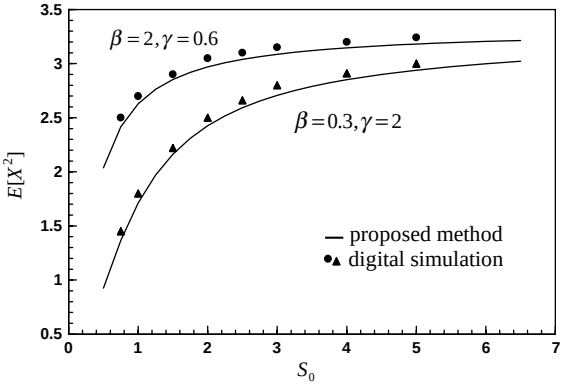

Fig. 7. Mean square displacement response versus excitation intensity ($e_1 = 1.0$, $e_2 = 0.0$, $\zeta = 0.2$, $k_1 = 2.0$, $k_3 = 0.03$, $\omega_g = 3.08$, $\zeta_g = 0.1$).

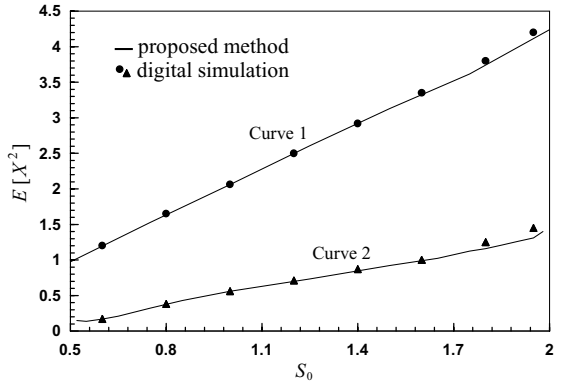

Fig. 9. Mean square displacement response versus excitation intensity (Curve 1: $e_1 = 1.0$, $e_2 = 0.12$, $\zeta = 0.2$, $k_1 = 2.0$, $k_3 = 0.03$, $\beta = 0.3$, $\gamma = 2.0$; Curve 2: $e_1 = 1.0$, $e_2 = 0.03$, $\zeta = 0.2$, $k_1 = 5.0$, $k_3 = 0.03$, $\beta = 0.1$, $\gamma = 3.0$).

the excitation filter. A favourable agreement between the results obtained by the proposed method and by the direct digital simulation is observed. The second case is the simultaneous external and parametric excitation by taking $e_1 = 1.0$ and $e_2 = 0.12$ and taking $e_1 = 1.0$ and $e_2 = 0.03$, respectively. Fig. 9 illustrates the mean square displacement response versus excitation intensity under the parameters $\omega_g = 3.08$ and $\zeta_g = 0.1$. A good coincidence between the results obtained by the two procedures is observed again. There is a slight increase of the difference when the excitation intensity increases.

5. Conclusions

In the present study an integrable Duhem hysteresis model is proposed to describe general hysteretic constitutive relationship. The proposed model covers a wide category of existing differential-type hysteresis models. Using the integrable Duhem hysteresis model, the conservative and dissipative parts of hysteretic force can be decoupled, and explicit expressions of hysteresis loop curves can be formulated. Random response analysis of the integrable Duhem hysteretic systems under external and/or parametric

non-white excitation is made by means of the stochastic averaging method of energy envelope. The total energy is approximated as a Markov diffusion process under the condition of weak damping and excitation. Space-averaging instead of time-averaging is performed to reduce the dimensionality of the concerned problem and to simplify the analytical solution procedure. The stationary probability density of total energy and the response statistics are obtained by solving the FPK equation associated with the averaged Itô equation of total energy, in which the Fourier series expansions are used to obtain explicit expressions of the drift and diffusion coefficients. A comparison of the response prediction results obtained by the proposed method and by the direct digital simulation verifies the accuracy of the proposed method.

Acknowledgements

This study was supported by The Hong Kong Polytechnic University through the Area of Strategic Development (ASD) Programme in Structural Engineering. The financial support by the National Science Foundation of China (Grant No. 19672054) to the second and fourth authors is also acknowledged.

Appendix A

A lot of commonly used differential-type hysteretic models can be derived from the proposed integrable Duhem hysteresis model. For example, the Bouc–Wen model [12,13]

$$z(t) = \kappa x(t) + r(t), \tag{A.1a}$$

$$\dot{r}(x) = \alpha\dot{x}(x) - \beta|\dot{x}(t)|r(t)|r(t)|^{n-1} - \gamma\dot{x}(t)|r(t)|^{n} \tag{A.1b}$$

can be obtained by taking the describing functions of the integrable Duhem hysteresis model as

$$z_{01}(x) = \kappa x, \tag{A.2a}$$

$$h_{x1}(x) = 1, \tag{A.2b}$$

$$h_{z1}(z - z_{01}) = \alpha - [\gamma + \beta\,\mathrm{sgn}(z - z_{01})]|z - z_{01}|^{n}, \tag{A.2c}$$

$$z_{02}(x) = \kappa x, \tag{A.2d}$$

$$h_{x2}(x) = 1, \tag{A.2e}$$

$$h_{z2}(z - z_{02}) = \alpha - [\gamma - \beta\,\mathrm{sgn}(z - z_{02})]|z - z_{02}|^{n}. \tag{A.2f}$$

For the Yar–Hammond bilinear model [8]

$$\dot{z}(t) = \dot{x}(t)\{\alpha - \gamma\,\mathrm{sgn}(\dot{x})\mathrm{sgn}[z - \beta\,\mathrm{sgn}(\dot{x})]\} \tag{A.3}$$

which corresponds to the integrable Duhem hysteresis model with the describing functions

$$z_{01}(x) = \beta, \tag{A.4a}$$

$$h_{x1}(x) = 1, \tag{A.4b}$$

$$h_{z1}(z - z_{01}) = \alpha - \gamma\,\mathrm{sgn}(z - z_{01}), \tag{A.4c}$$

$$z_{02}(x) = -\beta, \tag{A.4d}$$

$$h_{x2}(x) = 1, \tag{A.4e}$$

$$h_{z2}(z - z_{02}) = \alpha + \gamma\,\mathrm{sgn}(z - z_{02}). \tag{A.4f}$$

For the Dahl's friction model [44]

$$\dot{z}(x) = \sigma\dot{x}(t)\left|1 - \frac{z}{F_c}\,\mathrm{sgn}(\dot{x})\right|^{i} \times \mathrm{sgn}\left[1 - \frac{z}{F_c}\,\mathrm{sgn}(\dot{x})\right] \tag{A.5}$$

it has the describing functions as

$$z_{01}(x) = F_c, \tag{A.6a}$$

$$h_{x1}(x) = 1, \tag{A.6b}$$

$$h_{z1}(z - z_{01}) = -\sigma\left|\frac{z - z_{01}}{F_c}\right|^{i}\mathrm{sgn}\left[\frac{z - z_{01}}{F_c}\right], \tag{A.6c}$$

$$z_{02}(x) = -F_c, \tag{A.6d}$$

$$h_{x2}(x) = 1, \tag{A.6e}$$

$$h_{z2}(z - z_{02}) = \sigma\left|\frac{z - z_{02}}{F_c}\right|^{i}\mathrm{sgn}\left[\frac{z - z_{02}}{F_c}\right]. \tag{A.6f}$$

For the Coleman–Hodgdon ferromagnetic hysteresis model [45]

$$\dot{z}(x) = \dot{x}(t)\{\alpha\,\mathrm{sgn}(\dot{x})[f(x) - z] + g(x)\} \tag{A.7}$$

which corresponds to the integrable Duhem hysteresis model with the describing functions

$$z_{01}(x) = \mathrm{e}^{-\alpha x}\left\{c + \int [\alpha f(x) + g(x)]\mathrm{e}^{\alpha x}\,\mathrm{d}x\right\}, \tag{A.8a}$$

$$h_{x1}(x)h_{z1}(z - z_{01}) = 0, \tag{A.8b}$$

$$z_{02}(x) = -\mathrm{e}^{\alpha x}\{c + \int [-\alpha f(x) + g(x)]\mathrm{e}^{-\alpha x}\,\mathrm{d}x\}, \tag{A.8c}$$

$$h_{x2}(x)h_{z2}(z - z_{02}) = 0. \tag{A.8d}$$

Appendix B

The coefficients $a_i^{(k)}$, $b_i^{(k)}$, $c_i^{(k)}$ and $d_i^{(k)}$ $(k = 1, 2)$ in Eq. (23) are expressed as

$$a_i^{(1)} = \frac{2}{T}\int_0^T \sin\varphi f(H,\varphi)\cos\frac{2\pi i t}{T}\,\mathrm{d}t = -\frac{\sqrt{2}}{T\sqrt{H}}\int_0^T \dot{x} f(x,\dot{x})\cos\frac{2\pi i t}{T}\,\mathrm{d}t \tag{B.1a}$$

$$a_i^{(2)} = \frac{2}{T}\int_0^T \sin\varphi f(H,\varphi)\sin\frac{2\pi i t}{T}\,\mathrm{d}t = -\frac{\sqrt{2}}{T\sqrt{H}}\int_0^T \dot{x} f(x,\dot{x})\sin\frac{2\pi i t}{T}\,\mathrm{d}t \tag{B.1b}$$

$$b_i^{(1)} = \frac{2}{T}\int_0^T \cos\varphi f(H,\varphi)\cos\frac{2\pi i t}{T}\,\mathrm{d}t = \frac{2}{T\sqrt{H}}\int_0^T \mathrm{sgn}(x)\sqrt{U(x)} f(x,\dot{x}) \times\cos\frac{2\pi i t}{T}\,\mathrm{d}t \tag{B.1c}$$

$$b_i^{(2)} = \frac{2}{T}\int_0^T \cos\varphi f(H,\varphi)\sin\frac{2\pi i t}{T}\,\mathrm{d}t = \frac{2}{T\sqrt{H}}\int_0^T \mathrm{sgn}(x)\sqrt{U(x)} f(x,\dot{x}) \times\sin\frac{2\pi i t}{T}\,\mathrm{d}t \tag{B.1d}$$

$$c_i^{(1)} = \frac{2}{T}\int_0^T 2H\sin\varphi\frac{\partial f(H,\varphi)}{\partial H}\cos\frac{2\pi i t}{T}\,\mathrm{d}t = -\frac{2\sqrt{2}}{T\sqrt{H}}\int_0^T \dot{x}\left[\frac{\partial f(x,\dot{x})}{\partial x}\frac{U(x)}{\partial U(x)/\partial x} + \frac{\partial f(x,\dot{x})}{\partial \dot{x}}\frac{\dot{x}^2}{2}\right]\cos\frac{2\pi i t}{T}\,\mathrm{d}t \tag{B.1e}$$

$$c_i^{(2)} = \frac{2}{T}\int_0^T 2H\sin\varphi\frac{\partial f(H,\varphi)}{\partial H}\sin\frac{2\pi i t}{T}\,\mathrm{d}t = -\frac{2\sqrt{2}}{T\sqrt{H}}\int_0^T \dot{x}\left[\frac{\partial f(x,\dot{x})}{\partial x}\frac{U(x)}{\partial U(x)/\partial x} + \frac{\partial f(x,\dot{x})}{\partial \dot{x}}\frac{\dot{x}^2}{2}\right]\sin\frac{2\pi i t}{T}\,\mathrm{d}t \tag{B.1f}$$

$$d_i^{(1)} = \frac{2}{T}\int_0^T \sin\varphi\,\frac{\partial f(H,\varphi)}{\partial\varphi}\cos\frac{2\pi i t}{T}\,\mathrm{d}t = -\frac{2}{T\sqrt{H}}\int_0^T \mathrm{sgn}(x)\dot{x}\sqrt{U(x)} \times\left[\frac{\partial f(x,\dot{x})}{\partial x}\frac{\dot{x}}{\partial U(x)/\partial x} - \frac{\partial f(x,\dot{x})}{\partial \dot{x}}\right] \times\cos\frac{2\pi i t}{T}\,\mathrm{d}t \tag{B.1g}$$

$$d_i^{(2)} = \frac{2}{T}\int_0^T \sin\varphi\,\frac{\partial f(H,\varphi)}{\partial\varphi}\sin\frac{2\pi i t}{T}\,\mathrm{d}t = -\frac{2}{T\sqrt{H}}\int_0^T \mathrm{sgn}(x)\dot{x}\sqrt{U(x)} \times\left[\frac{\partial f(x,\dot{x})}{\partial x}\frac{\dot{x}}{\partial U(x)/\partial x} - \frac{\partial f(x,\dot{x})}{\partial \dot{x}}\right]\sin\frac{2\pi i t}{T}\,\mathrm{d}t \tag{B.1h}$$

$$i = 0, 1, 2, \ldots$$

in which,

$$\dot{x} = \pm\sqrt{2H - 2U(x)}, \tag{B.2a}$$

$$t = \int_{-a_1}^{x} \frac{\mathrm{d}x_1}{\pm\sqrt{2H - 2U(x_1)}}, \tag{B.2b}$$

$$T = 2\int_{-a_1}^{a_2} \frac{\mathrm{d}x}{\sqrt{2H - 2U(x)}}. \tag{B.2c}$$

References

[1] G.Q. Cai, Y.K. Lin, On randomly excited hysteretic structures, ASME J. Appl. Mech. 57 (1990) 442–448.

[2] I. Simulescu, T. Mochio, M. Shinozuka, Equivalent linearization method in nonlinear FEM, ASCE J. Eng. Mech. 115 (1989) 475–492.

[3] Y.K. Wen, Methods of random vibration for inelastic structures, Appl. Mech. Rev. 42 (1989) 39–52.

[4] R.D. Hanson, I.D. Aiken, D.K. Nims, P.J. Richter, R.E. Bachman, State-of-the-art and state-of-the-practice in seismic energy dissipation, Proceedings of the Seminar on Seismic Isolation, Passive Energy Dissipation, and Active Control, Report ATC 17-1, Vol. II, San Francisco, CA, 1993, pp. 449–471.

[5] G.W. Housner, L.A. Bergman, T.K. Caughey, A.G. Chassiakos, R.O. Class, S.F. Masri, R.E. Skelton, T.T. Soong, B.F. Spencer, J.T.P. Yao, Structural control: past, present, and future, ASCE J. Eng. Mech. 123 (1997) 897–971.

[6] B.F. Spencer Jr., M.K. Sain, Controlling buildings: a new frontier in feedback, IEEE Control Systems Mag. 17 (6) (1997) 19–35.

[7] M.D. Symans, M.C. Constantinou, Semi-active control systems for seismic protection of structures: a state-of-the-art review, Eng. Struct. 21 (1999) 469–487.

[8] M. Yar, J.K. Hammond, Modeling and response of bilinear hysteretic systems, ASCE J. Eng. Mech. 113 (1987) 1000–1013.

[9] Y. Suzuki, R. Minai, Application of stochastic differential equations to seismic reliability analysis of hysteretic structures, Prob. Eng. Mech. 3 (1988) 43–52.

[10] P.C. Jennings, Periodic response of a general yielding structure, ASCE J. Eng. Mech. Div. 90 (1964) 131–163.

[11] W.D. Iwan, A distributed-element model for hysteresis and its steady-state dynamic response, ASME J. Appl. Mech. 33 (1966) 893–900.

[12] R. Bouc, Forced vibration of mechanical systems with hysteresis, Proceedings of the Fourth Conference on Non-Linear Oscillation, Prague, Czechoslovakia, 1967, pp. 315–315.

[13] Y.K. Wen, Method for random vibration of hysteretic systems, ASCE J. Eng. Mech. Div. 102 (1976) 249–263.

[14] M.A. Bhatti, K.S. Pister, A dual criteria approach for optimal design of earthquake-resistant structural systems, Earthquake Eng. Struct. Dyn. 9 (1981) 557–572.

[15] J.L. Beck, P. Jayakumar, Class of masing models for plastic hysteresis in structures, in: S.K. Ghosh, J. Mohammadi (Eds.), Building an International Community of Structural Engineers, Vol. II, ASCE, New York, 1996, pp. 1083–1090.

[16] K.-C. Tsai, H.-W. Chen, C.-P. Hong, Y.-F. Su, Design of steel triangular plate energy absorbers for seismic-resistant construction, Earthquake Spectra 9 (1993) 505–528.

[17] M. Kikuchi, I.D. Aiken, An analytical hysteresis model for elastomeric seismic isolation bearings, Earthquake Eng. Struct. Dyn. 26 (1997) 215–231.

[18] H.R. Lo, J.K. Hammond, M.G. Sainsbury, Nonlinear system identification and modelling with application to an isolator with hysteresis, Proceedings of the Sixth International Modal Analysis Conference, Vol. II, Kissimmee, FL, 1988, pp. 1453–1459.

[19] N. Mostaghel, Analytical description of pinching, degrading hysteretic systems, ASCE J. Eng. Mech. 125 (1999) 216–224.

[20] G.F. Demetriades, M.C. Constantinou, A.M. Reinhorn, Study of wire rope systems for seismic protection of equipment in buildings, Eng. Struct. 15 (1993) 321–334.

[21] Y.Q. Ni, J.M. Ko, C.W. Wong, S. Zhan, Modelling and identification of a wire-cable vibration isolator via a cyclic loading test, Part 1: experiments and model development, Inst. Mech. Engrs. J. Systems Control Eng. 213 (1999) 163–171.

[22] T.K. Caughey, Random vibration of system with bilinear hysteresis, ASME J. Appl. Mech. 27 (1960) 649–652.

[23] K. Asano, W.D. Iwan, An alternative approach to the random response of bilinear hysteretic systems, Earthquake Eng. Struct. Dyn. 12 (1984) 229–236.

[24] J.B. Roberts, Application of averaging methods to randomly excited hysteretic systems, in: F. Ziegler, G.I. Schuëller (Eds.), Nonlinear Stochastic Dynamic Engineering Systems, Springer, Berlin, 1988, pp. 361–379.

[25] W.Q. Zhu, Y. Lei, Stochastic averaging of energy envelope of bilinear hysteretic system, in: F. Ziegler, G.I. Schuëller (Eds.), Nonlinear Stochastic Dynamic Engineering Systems, Springer, Berlin, 1988, pp. 381–391.

[26] P.K. Koliopulos, E.A. Nichol, G.D. Stefanou, Some aspects of the statistics of a bilinear hysteretic structure under a non-white random excitation, Computer Methods Appl. Mech. Eng. 110 (1993) 57–61.

[27] H. Takemiya, L.D. Lutes, Stationary random vibration of hysteretic systems, ASCE J. Eng. Mech. Div. 103 (1977) 673–687.

[28] P.-T.D. Spanos, Hysteretic structural vibrations under random load, J. Acoust. Soc. Am. 65 (1979) 404–410.

[29] Y.K. Wen, Equivalent linearization for hysteretic systems under random excitation, ASME J. Appl. Mech. 47 (1980) 150–154.

[30] T.T. Baber, M.N. Noori, Random vibration of degrading, pinching systems, ASCE J. Eng. Mech. 111 (1985) 1010–1026.

[31] H.J. Pradlwarter, G.I. Schuëller, Equivalent linearization—a suitable tool for analyzing MDOF-systems, Prob. Eng. Mech. 8 (1993) 115–126.

[32] F. Casciati, L. Faravelli, P. Venini, Frequency analysis in stochastic linearization, ASCE J. Eng. Mech. 120 (1994) 2498–2518.

[33] G.C. Foliente, M.P. Signh, M.N. Noori, Equivalent linearization of generally pinching hysteretic, degrading systems, Earthquake Eng. Struct. Dyn. 25 (1996) 611–629.
[34] W.Q. Zhu, Y.K. Lin, Stochastic averaging of energy envelope, ASCE J. Eng. Mech. 117 (1991) 1890–1905.
[35] M. Noori, M. Dimentberg, Z. Hou, R. Christodoulidou, A. Alexandrou, First-passage study and stationary response analysis of a BWB hysteresis model using quasi-conservative stochastic averaging method, Prob. Eng. Mech. 10 (1995) 161–170.
[36] J.W. Macki, P. Nistri, P. Zecca, Mathematical models for hysteresis, SIAM Rev. 35 (1993) 94–123.
[37] M.A. Krasnoselskii, A.V. Pokrovskii, Systems with Hysteresis, Springer, Berlin, 1989.
[38] I.D. Mayergoyz, Mathematical Models of Hysteresis, Springer, New York, 1991.
[39] A. Visintin, Differential Models of Hysteresis, Springer, Berlin, 1994.
[40] Y.Q. Ni, J.M. Ko, C.W. Wong, Nonparametric identification of nonlinear hysteretic systems, ASCE J. Eng. Mech. 125 (1999) 206–215.
[41] W.Q. Zhu, Y. Lei, Equivalent nonlinear system method for stochastically excited and dissipated integrable Hamiltonian systems, ASME J. Appl. Mech. 64 (1997) 209–216.
[42] G.Q. Cai, Random vibration of nonlinear system under nonwhite excitation, ASCE J. Eng. Mech. 121 (1995) 633–639.
[43] G.Q. Cai, Y.K. Lin, Random vibration of strongly nonlinear systems, Nonlinear Dyn. 24 (2001) 3–15.
[44] P.K. Dahl, Solid friction damping of mechanical vibrations, AIAA J. 14 (1976) 1675–1682.
[45] B.D. Coleman, M.L. Hodgdon, A constitutive relation for rate-independent hysteresis in ferromagnetically soft materials, Int. J. Eng. Sci. 24 (1986) 897–919.